Università di Pisa

Modeling End-of-the-Roadmap CMOS Devices

Gilberto Curatola
Dipartimento di Ingegneria dell'Informazione: Elettronica, Informatica, Telecomunicazioni, Università di Pisa
Gianluca Fiori
Dipartimento di Ingegneria dell'Informazione: Elettronica, Informatica, Telecomunicazioni, Università di Pisa
Giuseppe Iannaccone
Dipartimento di Ingegneria dell'Informazione: Elettronica, Informatica, Telecomunicazioni, Università di Pisa

G. Curatola, G. Fiori, G. Iannaccone, *Modeling End-of-the-Roadmap CMOS Devices*, Workshop on the Ultimate Integration of Silicon, 20-21 March 2003, Udine.

Modeling End-of-the-Roadmap CMOS devices

G. Curatola, G. Fiori, G. Iannaccone

Dipartimento di Ingegneria dell'Informazione,

Università degli Studi di Pisa
Via Diotisalvi 2, I-56122, Pisa, Italy.

Acknowledgments:

- **EU - IST 1999-10828 NANOTCAD**
- **Fondazione CRP**

Motivation

- In MOSFETs, the fraction of carriers traversing the channel without suffering inelastic scattering ("ballistic") is expected to predominate over electrons undergoing phonon scattering for channel lengths shorter than 30 nm (Bude 2000, Lundstrom 2000).
- Simulation tools of nanoscale MOSFETs should consider ballistic electrons as mainstream electrons, and thermalized electrons with a perturbative approach
- The same tools should also allow to take into account in a selfconsistent way:
  - ✓ Strong quantum confinement in the channel
  - ✓ Gate leakage
  - ✓ Atomistic Effects
  - ✓ Source to drain tunneling
  - ✓ The effect of strain (for SiGe/Si devices)
- Commercial TCAD tools are not yet adequate

Fully ballistic transport

- Electrons emitted from the source with sufficient energy to overcome the barrier in the channel reach the drain conserving energy and transversal momentum

- Electron states originating from the source (drain) obey the Fermi-Dirac statistics with source (drain) Fermi Energy Efs (Efd).

- This ensures continuity of current density per unit energy in each subband

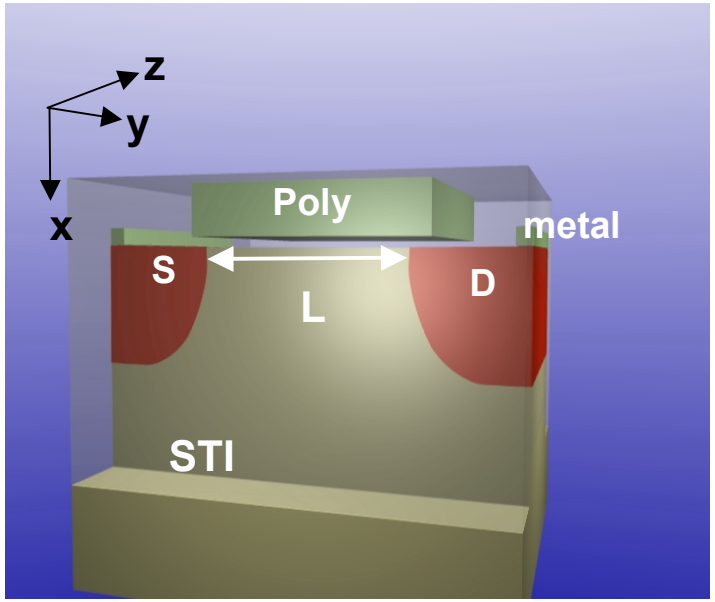

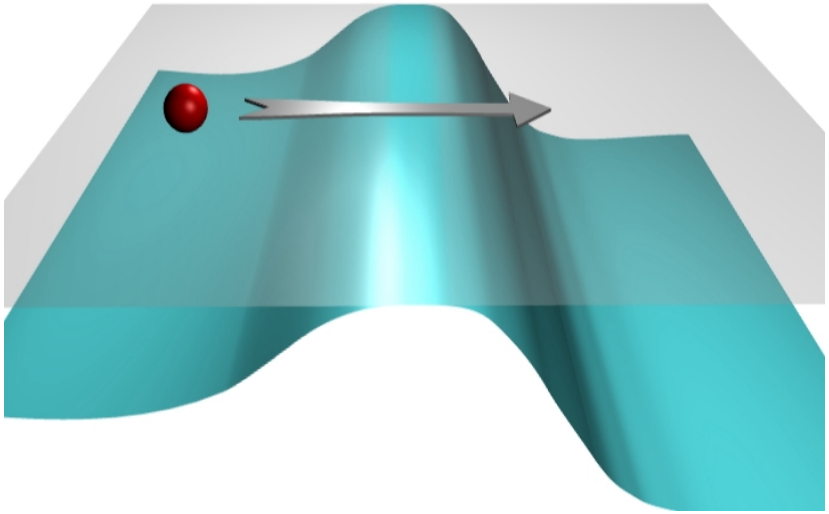

3D Poisson-Schrödinger solver (I)

$$\nabla[\varepsilon\nabla\phi(\vec{r})] = -q[-n(\phi) + p(\phi) - N_A^-(\phi) + N_D^+(\phi)]$$

- 1st step: Poisson non-linear equation in 3D
- The strong confinement limited to the *x* direction, perpendicular to the Si/SiO_2 interface, allows us to decouple the Schrödinger equation into
  - ✓ a 1D equation in the *x* direction,
  - ✓ a 2D equation in the *y*-*z* plane. The density of states in the *y*-*z* plane is well approximated by the semiclassical expression.
- The single particle Schrödinger equation in 3D reads

$$(\hat{T}_x + \hat{T}_y + \hat{T}_z)\Psi + E_C(x,y,z)\Psi = E\Psi$$

3D Poisson-Schrödinger solver (II)

- We can write Ψ as $\Psi(x,y,z) = \psi(x,y,z)\chi(y,z)$
- where ψ is the solution of

$$\hat{T}_x \psi + E_C(x,y,z)\psi = \widetilde{E}(y,z)\psi$$

- The Schrödinger equation becomes

$$(\hat{T}_y + \hat{T}_z)\chi\psi = [E - \widetilde{E}(y,z)]\chi\psi$$

- Assuming that ψ is weakly dependent on *y* and *z*, we have

$$(\hat{T}_y + \hat{T}_z)\chi = [E - \widetilde{E}(y,z)]\chi$$

- Since $\widetilde{E}(y,z)$ is rather smooth, χ is well approximated by the semiclassical density of states.

Decoupling the Schrödinger equation

$$\delta = \max_{y,z} \left| \frac{(\hat{T}_y + \hat{T}_z)\psi\chi - \psi(\hat{T}_y + \hat{T}_z)\chi}{[E - \tilde{E}(y,z)]\psi\chi} \right|$$

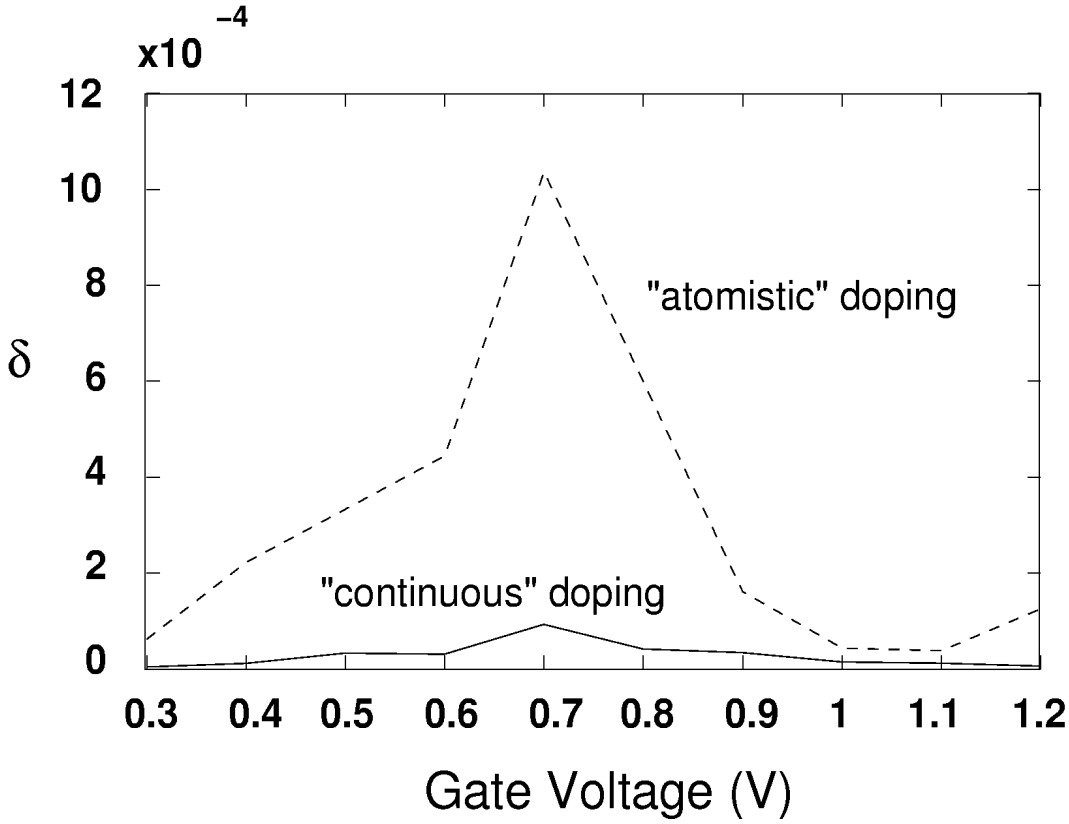

- δ is the norm infinity of the relative error on the eigenvalue introduced by our approximation
- We plot δ as a function of the gate voltage for the 25 nm MOSFET
- In order to consider the worst case, δ is plotted in the case of "atomistic" doping
- δ is always << 1

Mass anisotropy and electron density

- **The Schrödinger equation must be solved twice:**
  - ✓ **For the 2 minima along the vertical (x) direction**

$$-\frac{\hbar^2}{2}\left[\frac{\partial}{\partial x}\frac{1}{m_l}\frac{\partial}{\partial x}\Psi_{li}(x,y)\right]+E_C\Psi_{li}=\tilde{E}_{li}(y)\Psi_{li}$$

$$n_{li}=\frac{k_B T m_t}{\pi\hbar^2}\left|\Psi_{li}\right|^2 ln\left[1+exp\left(-\frac{\tilde{E}_{li}-E_F}{k_B T}\right)\right]$$

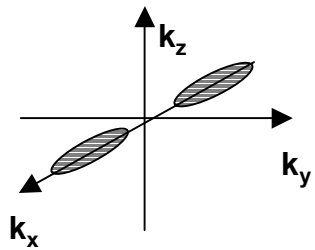

  - ✓ **For the other 4 minima**

$$-\frac{\hbar^2}{2}\left[\frac{\partial}{\partial x}\frac{1}{m_t}\frac{\partial}{\partial x}\Psi_{ti}(x,y)\right]+E_C\Psi_{ti}=\tilde{E}_{ti}(y)\Psi_{ti}$$

$$n_{ti}=\frac{k_B T\sqrt{m_l m_t}}{\pi\hbar^2}\left|\Psi_{ti}\right|^2 ln\left[1+exp\left(-\frac{\tilde{E}_{ti}-E_F}{k_B T}\right)\right]$$

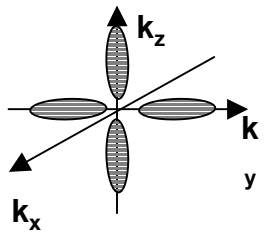

  - ✓ **The quantum electron density becomes**

$$n=\sum_i 2n_{li}+\sum_i 4n_{ti}$$

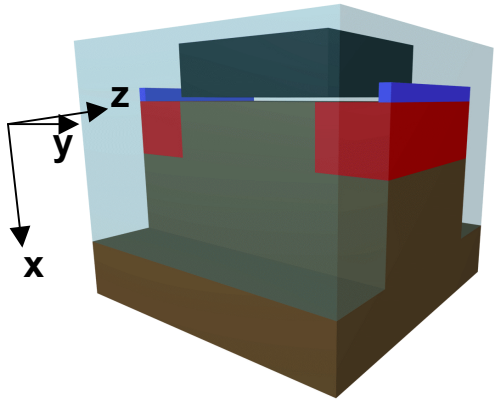

Model out of equilibrium

- Let E_{imax} be the maximum of the *i*-th subband in the channel, and $D_l(E_y)$ the longitudinal density of states
  - ✓ In the *i*-th subband, on the left of the subband peak, we have:

$$n_{li} = |\Psi_{li}|^2 \int_0^{E_{i\,max}-\tilde{E}_i} D_l(E_y) f(E_y + \tilde{E}_i - E_{FS}) dE_y$$

$$+ |\Psi_{li}|^2 \int_{E_{i\,max}-\tilde{E}_i}^{\infty} D_l(E_y) \left[\frac{f(E_y + \tilde{E}_i - E_{FS}) + f(E_y + \tilde{E}_i - E_{FD})}{2} \right] dE_y$$

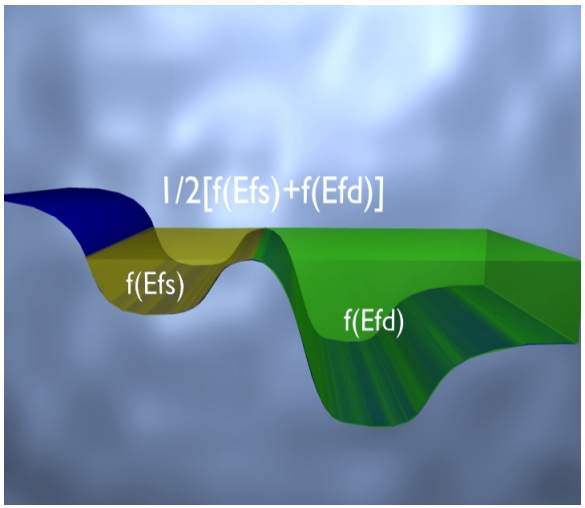

- We have $n = \sum_i 2n_{li} + \sum_i 4n_{ti}$
- Continuity of current density per unit energy is ensured in each subband

Model out of equilibrium

- **When the Poisson-Schrödinger equation is solved (NR), and charge density and potential profiles are known, we compute the current density in the i-th subband**

$$J_{li} = q\Gamma\left(\tfrac{1}{2}\right)\frac{\sqrt{2m_t kT}}{h^2}\int_{E_{i\,max}-\widetilde{E}_{li}}^{\infty}\left[F_{-1/2}\left(-\frac{\widetilde{E}_{li}+E_y-E_{FS}}{kT}\right)-F_{-1/2}\left(-\frac{\widetilde{E}_{li}+E_y-E_{FD}}{kT}\right)\right]dE_y$$

- **The total current density is**

$$J = 2\sum_i J_{li} + 2\sum_i J_{lti} + 2\sum_i J_{tti}$$

“Well tempered” MOSFETs

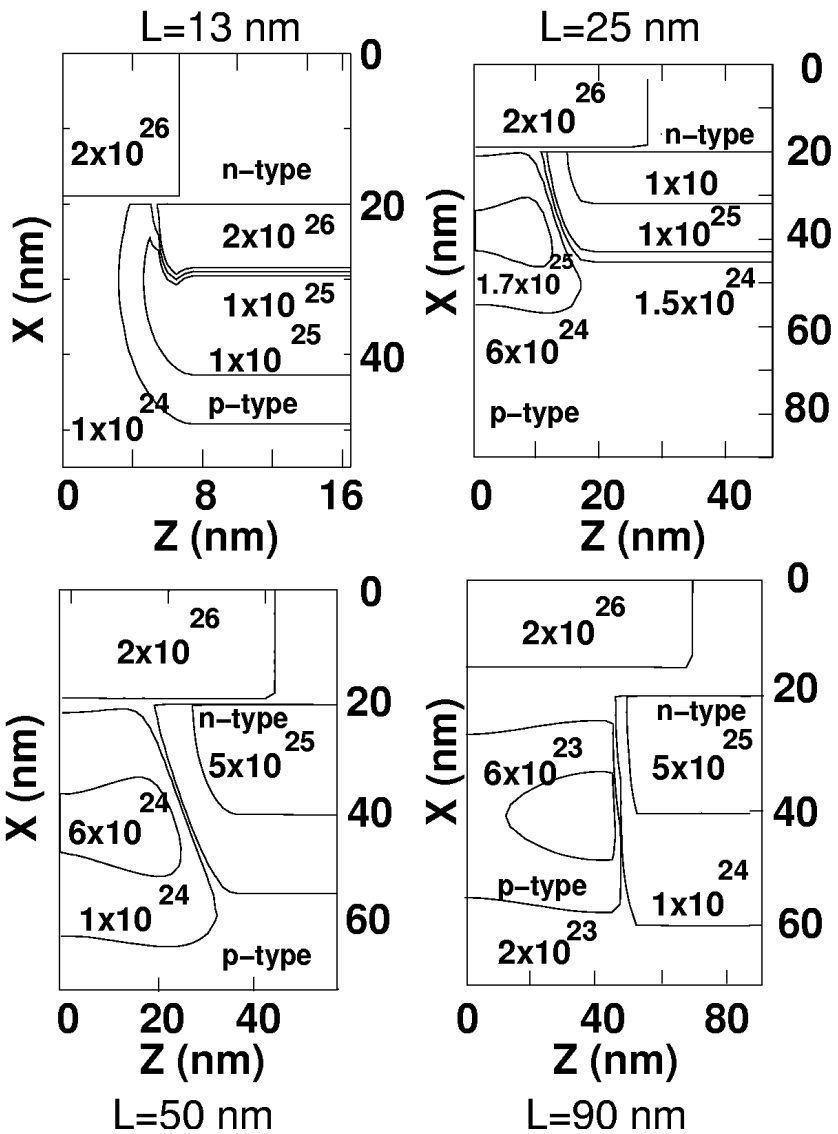

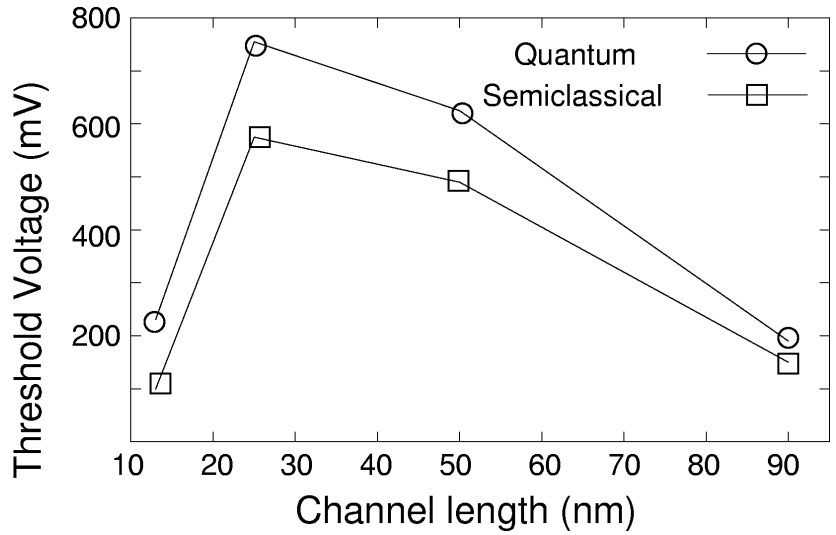

- **www.ece.mit.edu/Well**
- **L=13 nm, L=25 nm, L=50 nm, L=90 nm**
- **Maximum ΔV_T = 170 mV**

25 nm MOSFET

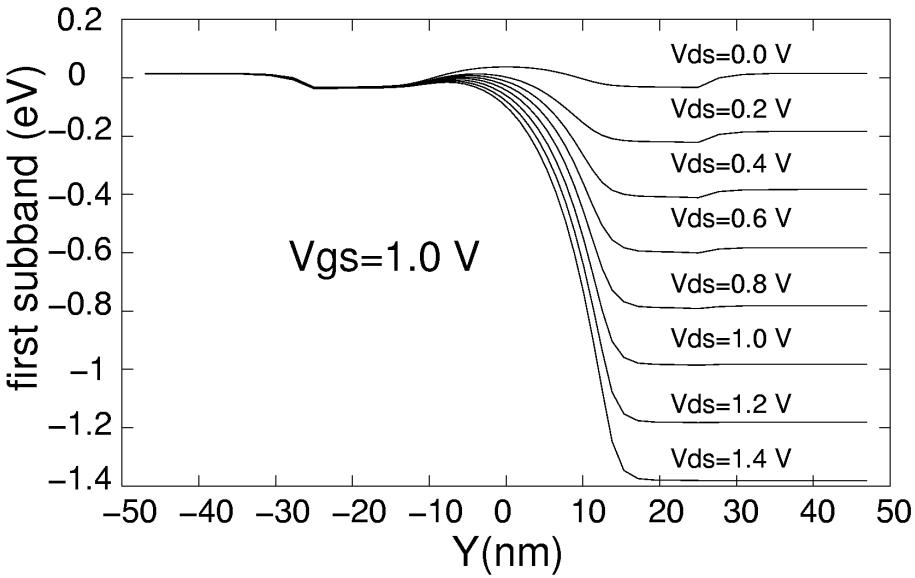

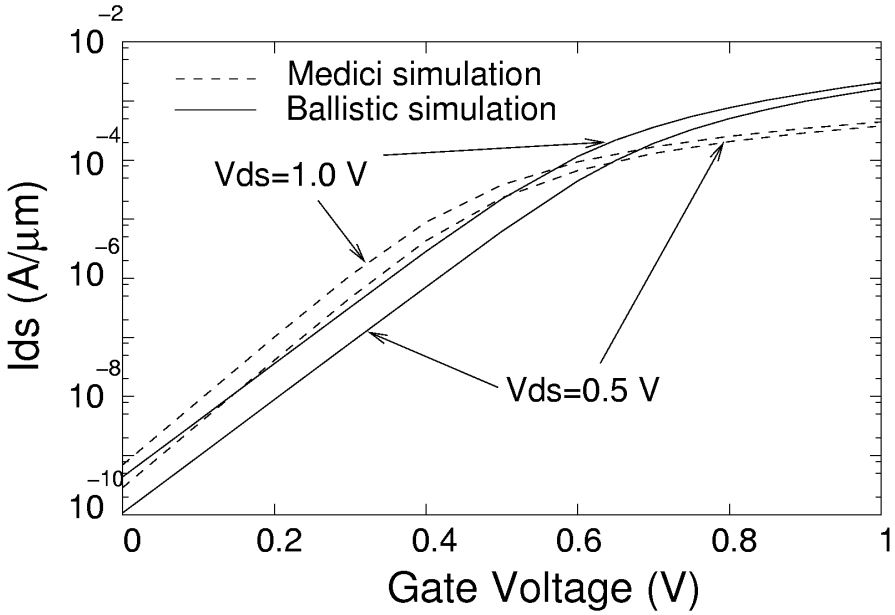

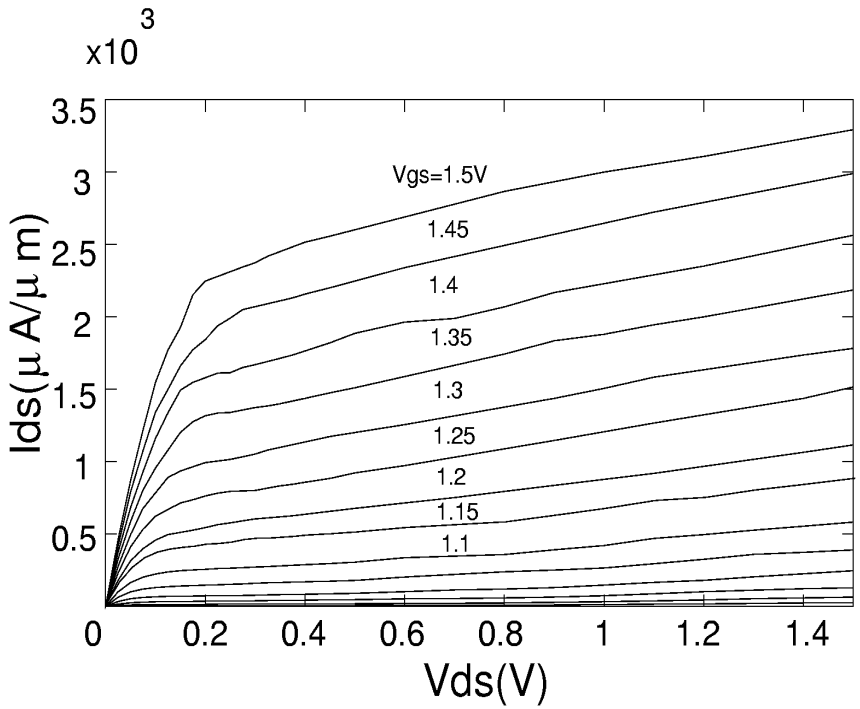

- **2D simulation**
- **First subband profile in the longitudinal direction for increasing Vds.**

Ultra-thin SOI MOSFETs

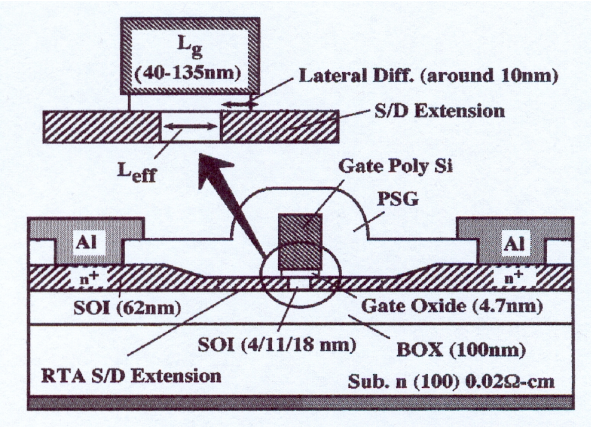

E.Suzuki, et al., IEEE-TED 2000

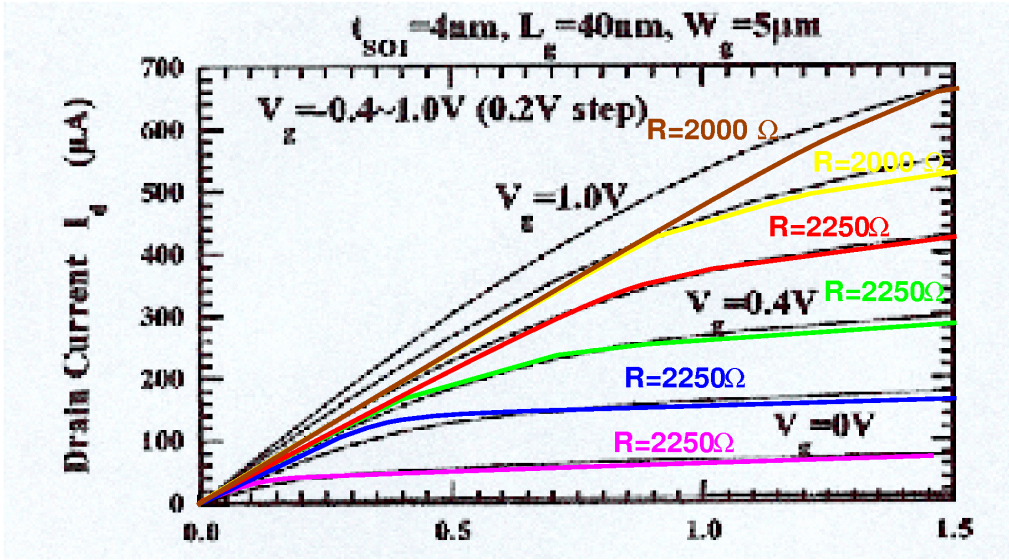

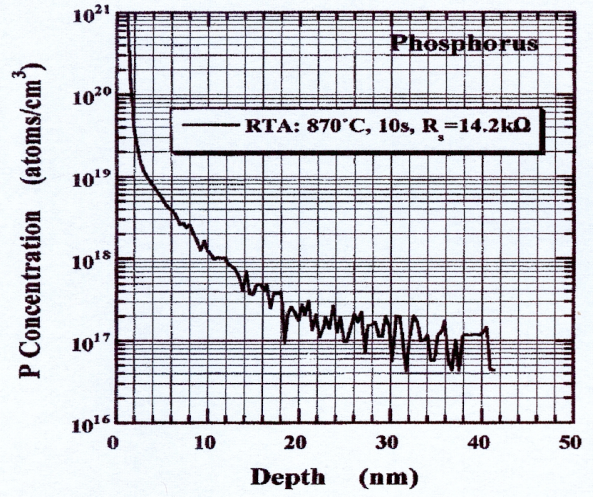

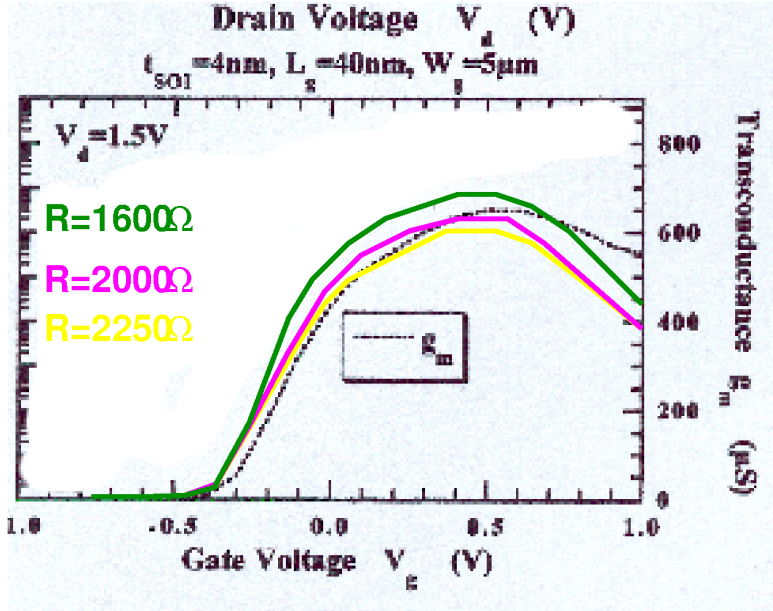

- In color: theoretical curves

Thanks: C.Berti

Strain-induced degeneracy lifting

- Stress causes a splitting of the six fold degenerate conduction band into two-fold and four-fold degenerate valleys.
- Reduced intervalley scattering.

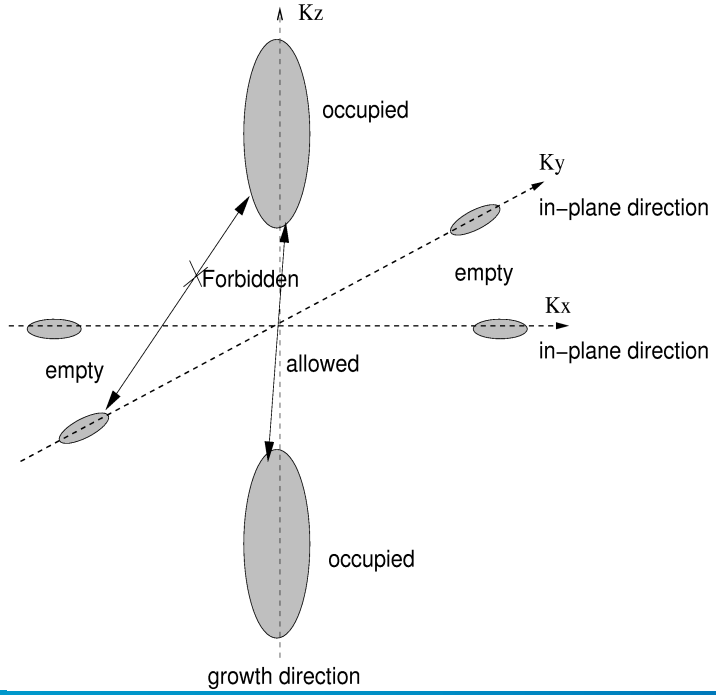

- Lifting of the valence band degeneracy at the Γ point. While heavy holes are at the valence band edge under biaxial compressive strain (x > y), light holes are at the valence band edge for tensile strain (x< y).

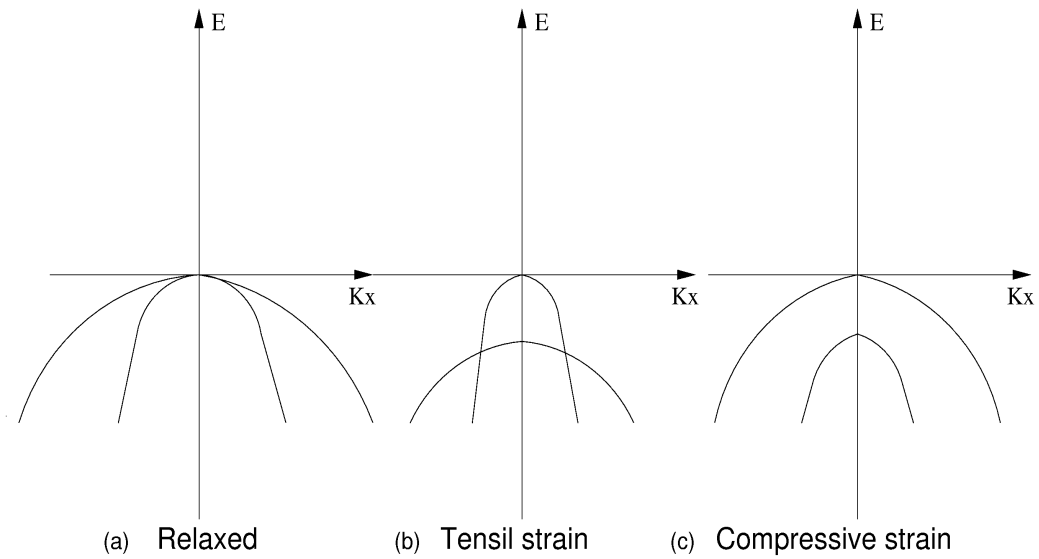

Silicon-Germanium MOSFETs

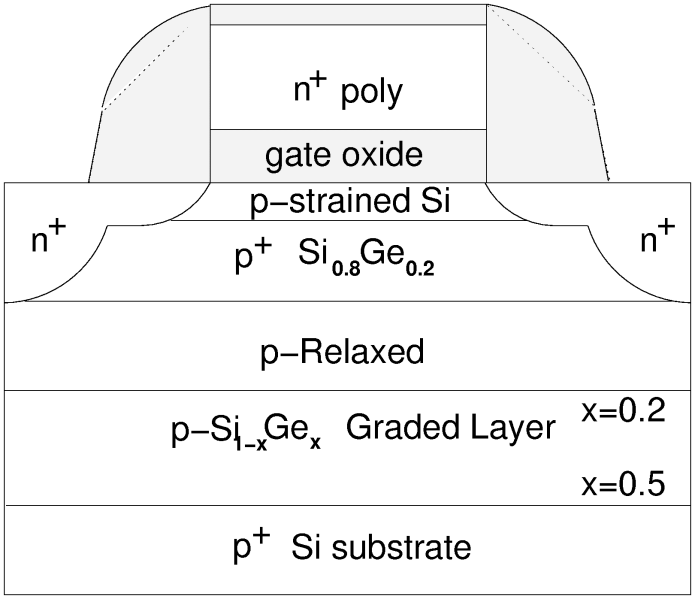

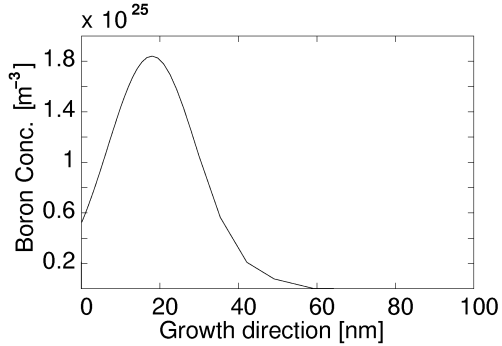

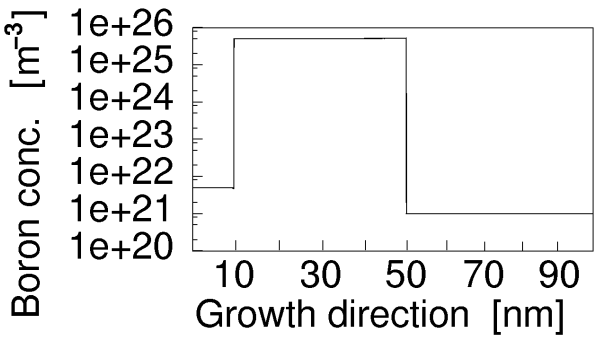

- **25 nm SiGe MOSFET with 10 nm strained-Si channel on a $Si_{0.8}Ge_{0.2}$ virtual substrate.**
- **The rest of the structure is identical to the previous "Well tempered" 25 nm MOSFET**

- **Two doping profiles have been considered**
  - ✓ **The super-halo doping of the 25 nm well-tempered**
  - ✓ **Epi-doping of 5 x10^{19} cm^{-3}**

Comparison between bulk Si and strained Si MOSFETs (n-type)

- **Note: in this regime, mobility has no physical meaning**
- ***No improvement of current drive is observed in SiGe*** **(preliminary)**

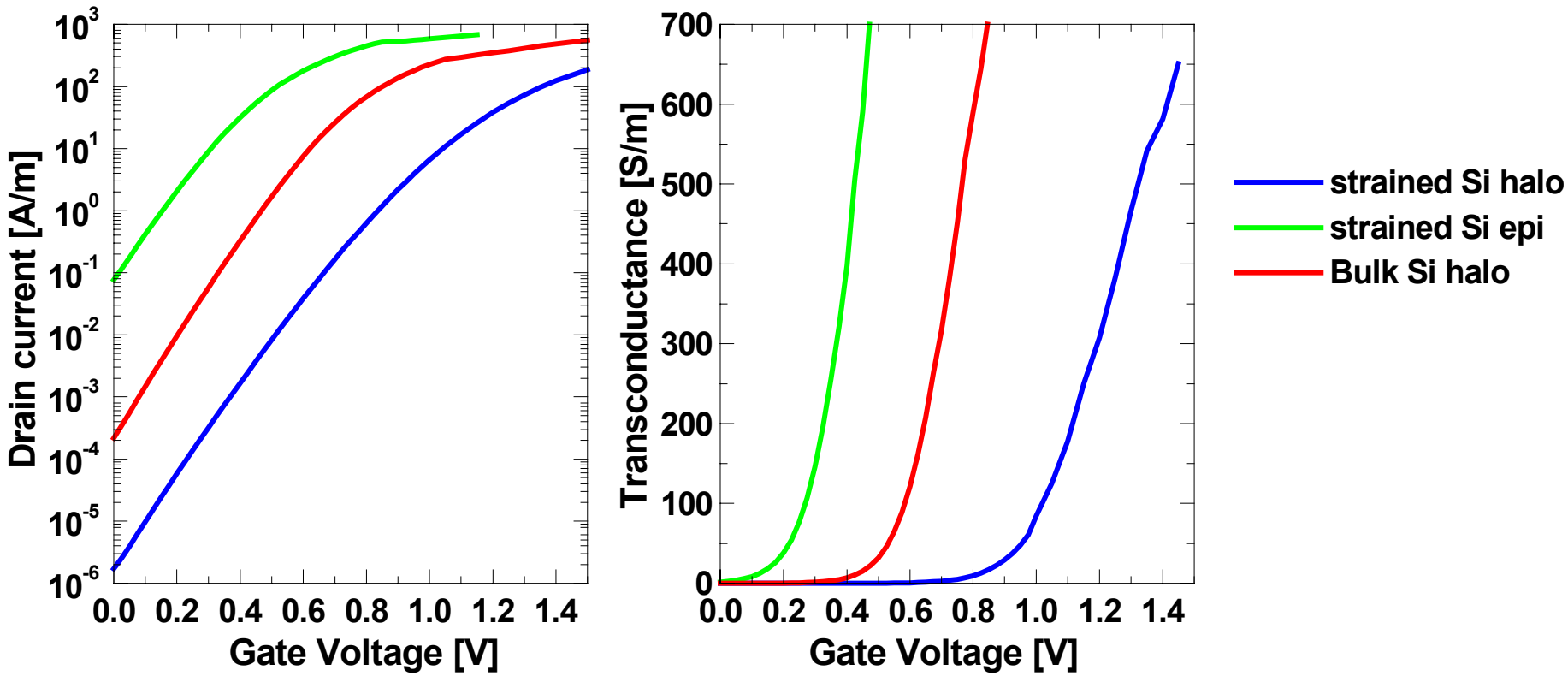

Partially ballistic transport: Coupling 2D PS and BTE

- **We assume that electrons in each 2D subband can be described by Boltzmann Transport Equation**
- **Initial guess: subband profiles are obtained with the 2D PS solver assuming ballistic transport.**
- **In each subband the BTE is directly solved (box integration)**
  - ✓ **Constant relaxation time, but can be easily extended to a general scattering term.**

$$v_y \frac{\partial F(y,k_y)}{\partial y} - \frac{qE_y}{\hbar}\frac{\partial F(y,k_y)}{\partial k_y} = \frac{F_{eq}(y,k_y) - F(y,k_y)}{\tau}$$

  - ✓ **The BTE can be easily solved since** $F = F(y,ky)$
- **The obtained charge density is used as a source term of the Poisson equation**
- **New subbands are obtained by solving the Schrödinger equation**

Partially ballistic transport

- Boltzmann Transport Equation solved in each 2D subband
- Direct solution (no Montecarlo) -

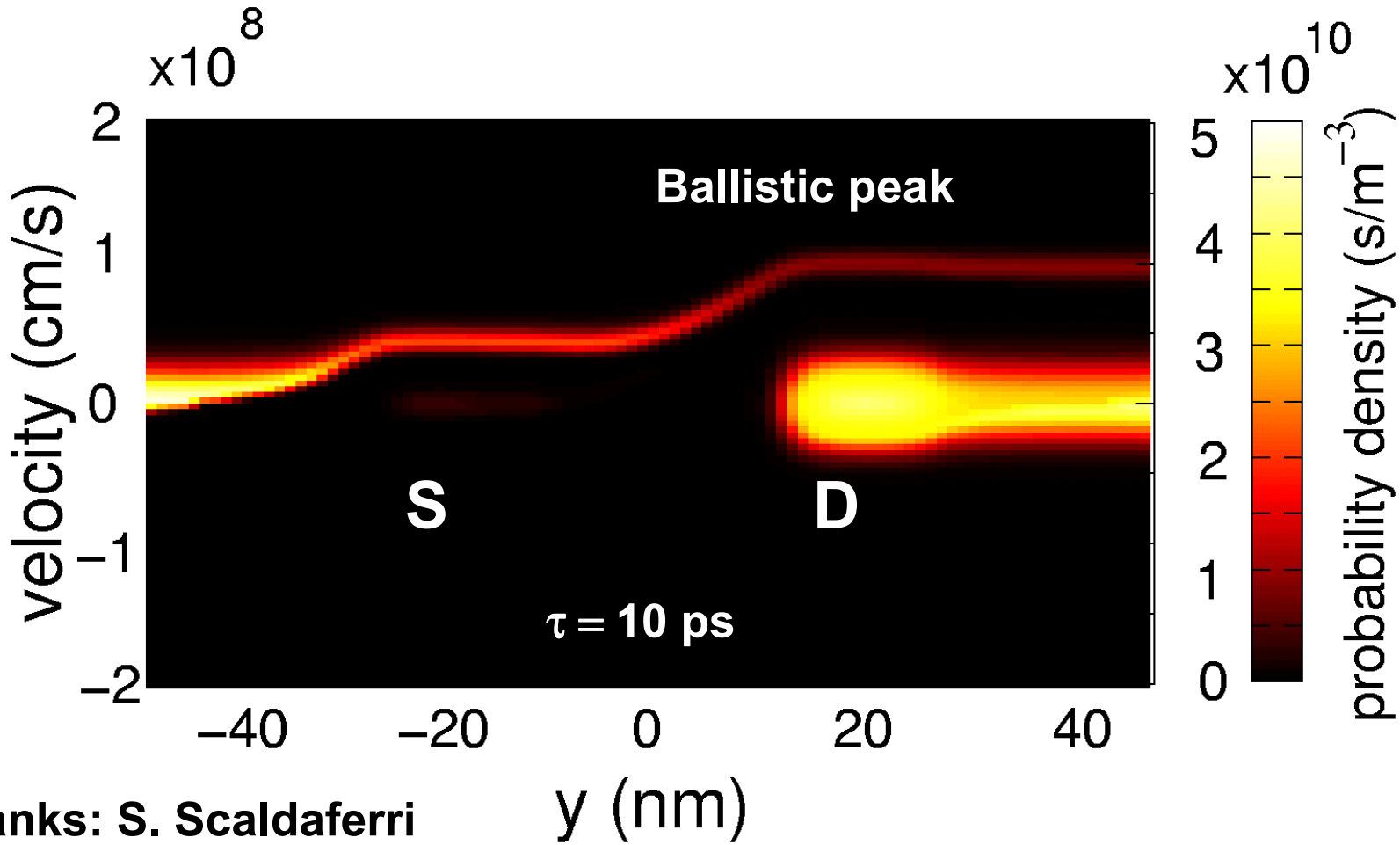

Thanks: S. Scaldaferri

Partially ballistic transport

- Boltzmann Transport Equation solved in each 2D subband
- Direct solution (no Montecarlo)

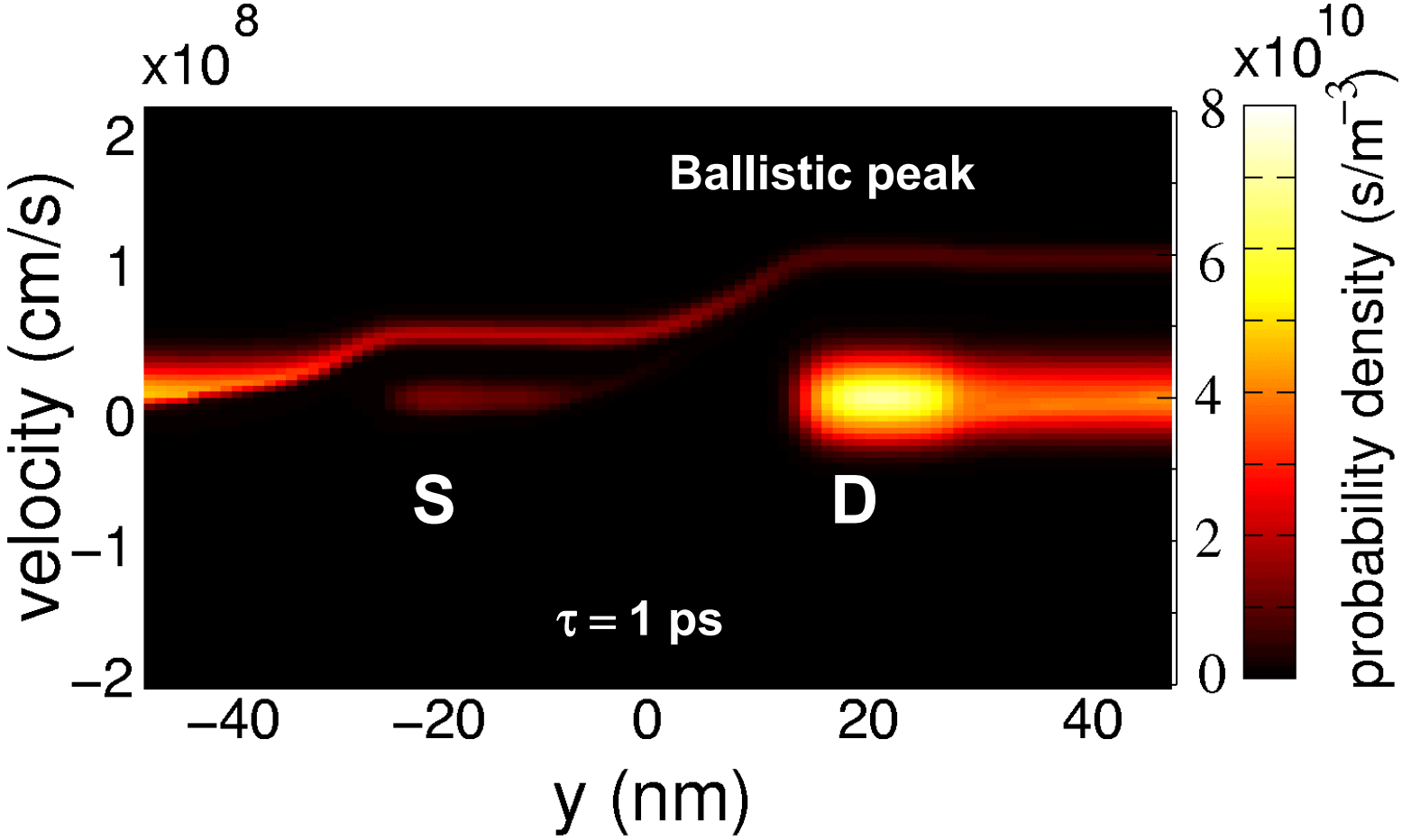

Partially ballistic transport

- Boltzmann Transport Equation solved in each 2D subband
- Direct solution (no Montecarlo)

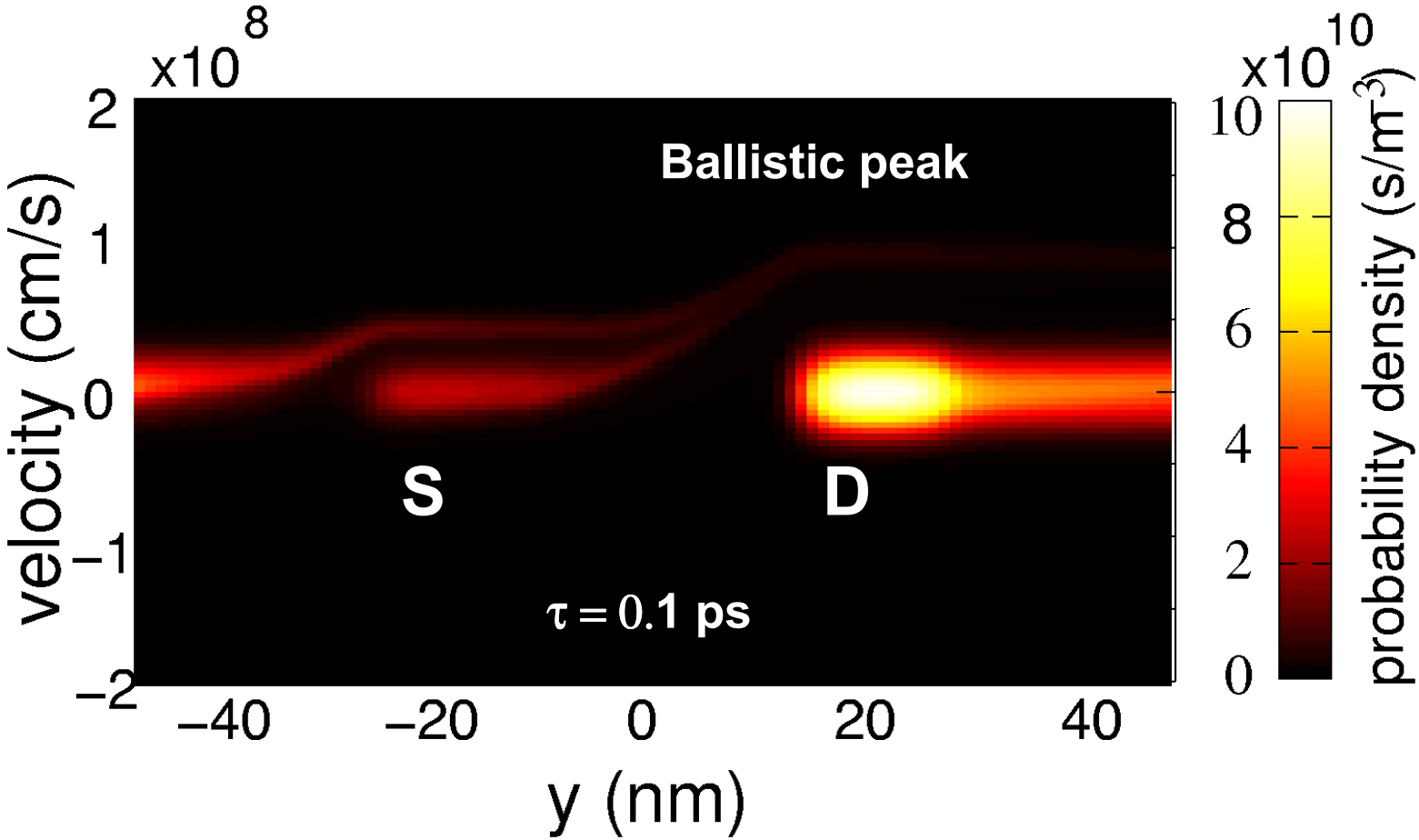

Partially ballistic transport

- Boltzmann Transport Equation solved in each 2D subband
- Direct solution (no Montecarlo)

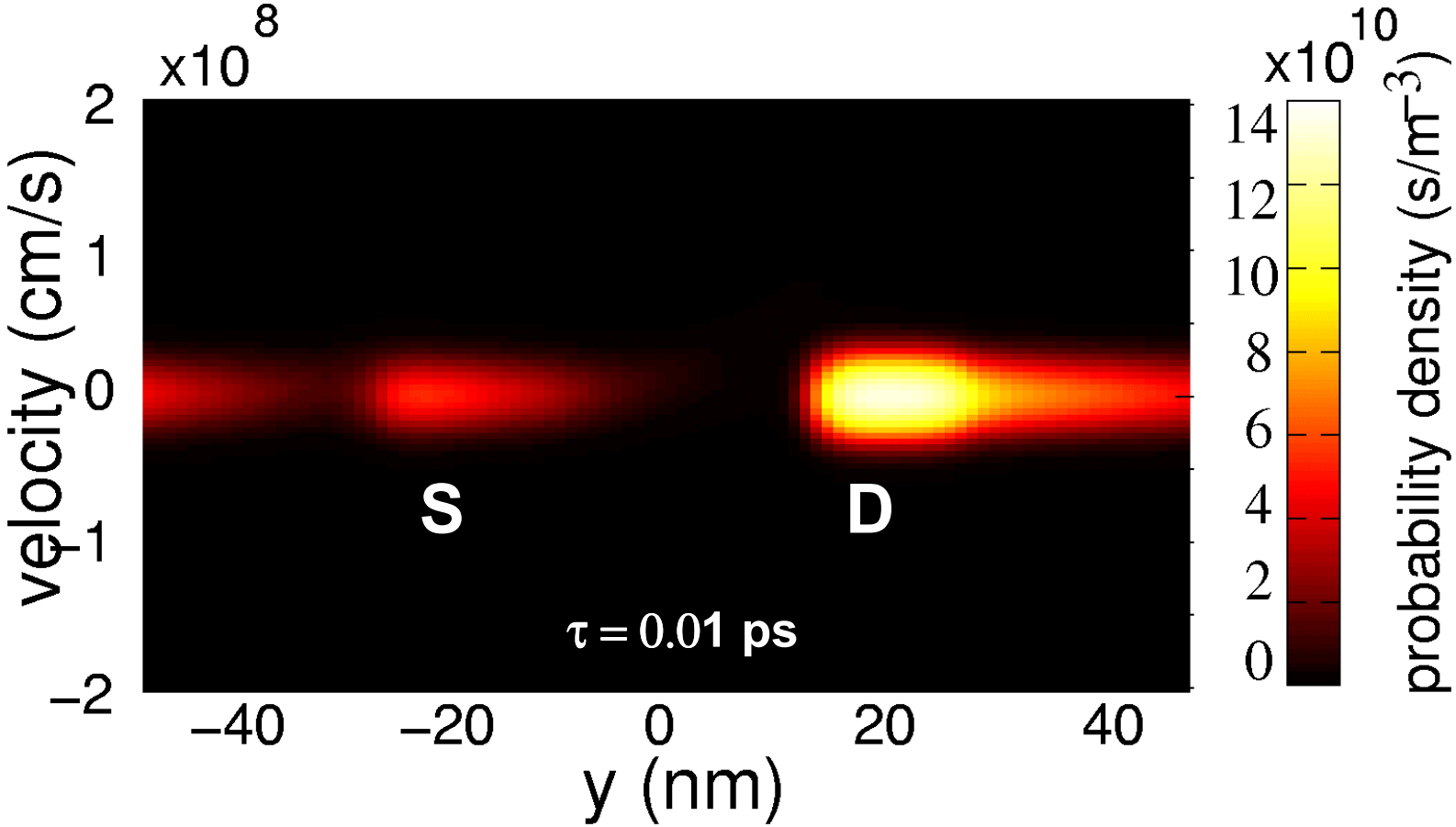

Current density per unit energy

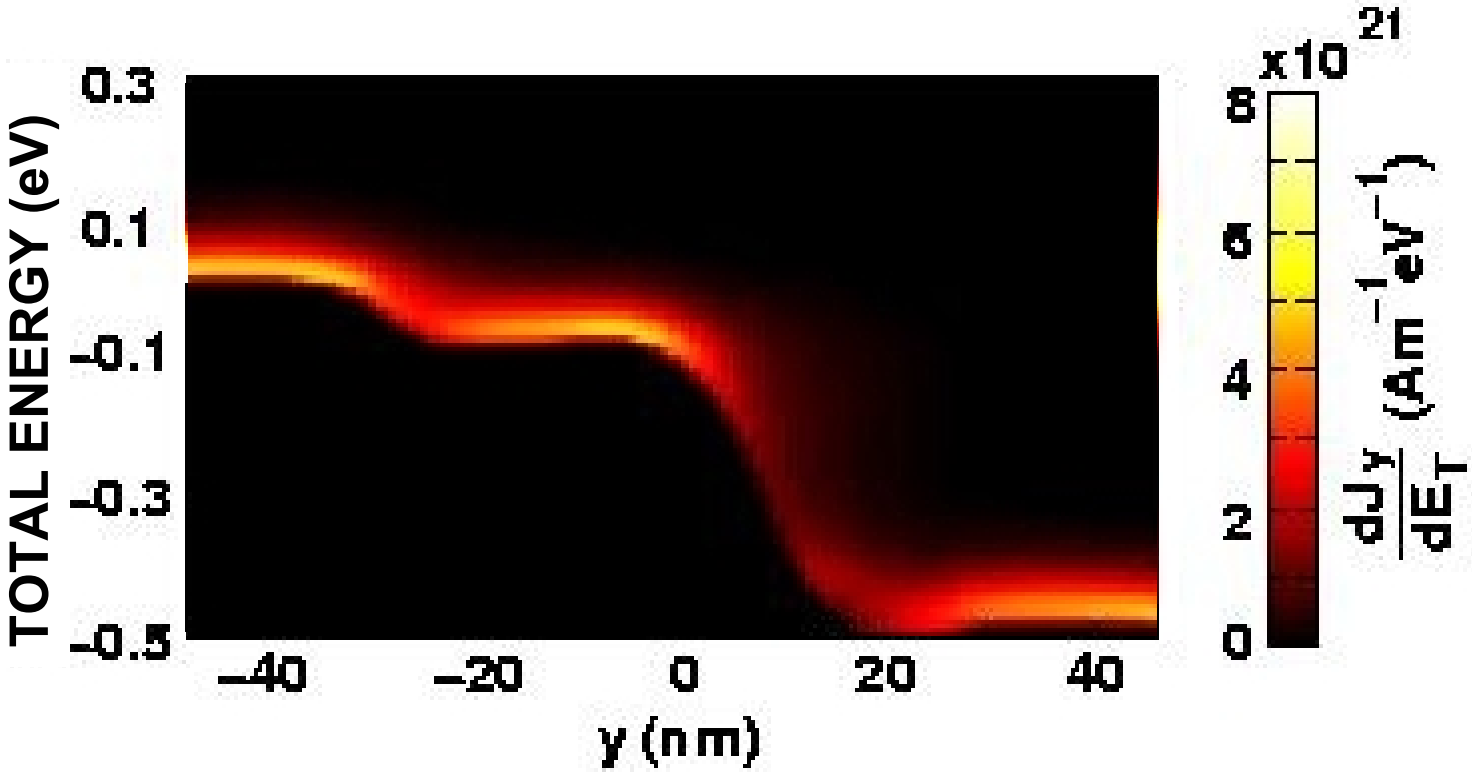

- **Scattering time**: 10^{-14} s

Partially ballistic transport

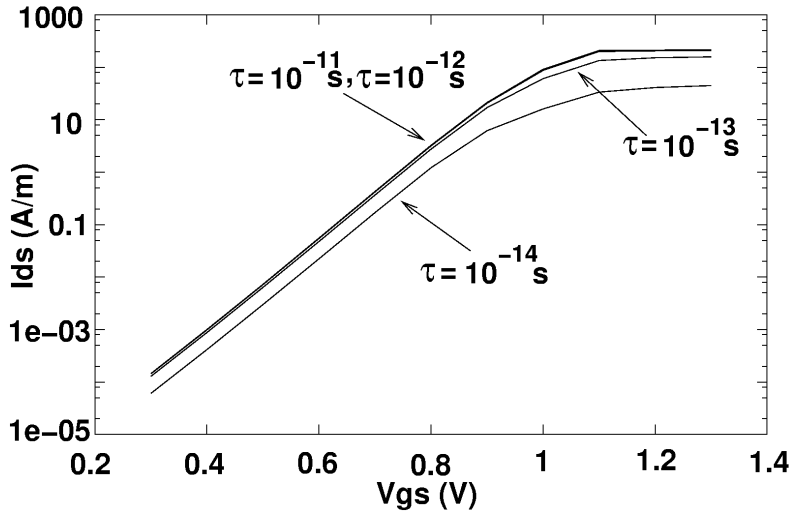

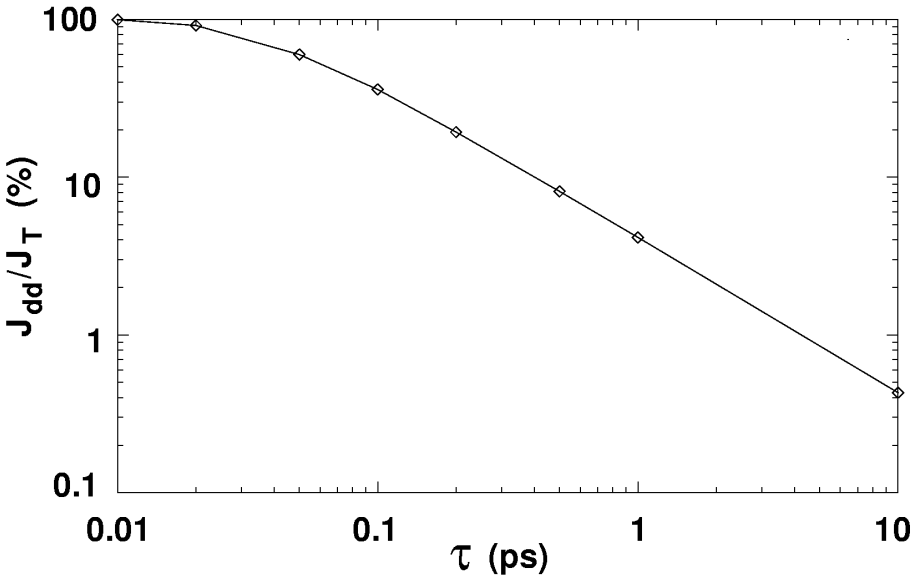

- Transfer characteristics
- Vds = 0.5 V

- Non-ballistic fraction of the total current at the drain.

Random dopant distribution

In the sub-100 nm regime, the number of impurity atoms is of the order of hundreds in the depletion region. Doping fluctuations are no longer negligible and determine the dispersion of electric quantities such as the threshold voltage.

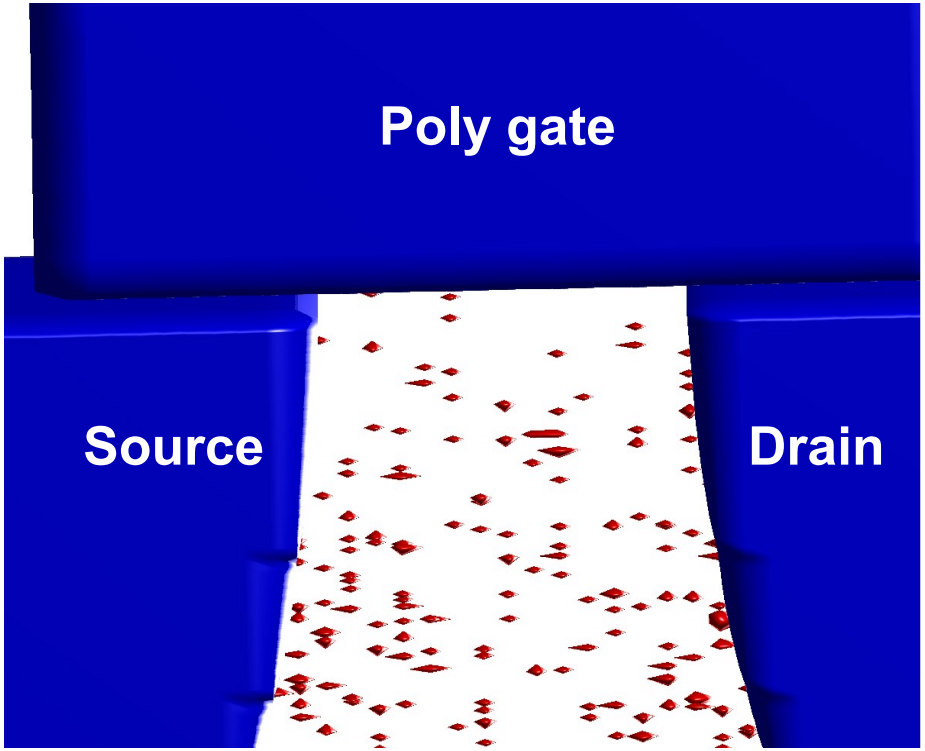

	Average number of dopants in the depletion region
W=90nm	107
W=50nm	398
W=25nm	217

Discrete distribution of dopants in the channel

1D modeling is not adequate for "realistic" decanano MOSFET

- Doping profiles are highly inhomogeneous in the plane
- Correlation between M and V_T is poor for the 25 nm MOSFET

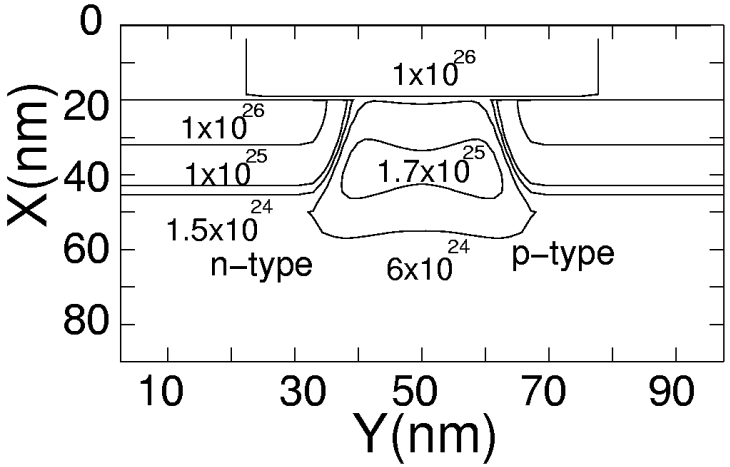

$$M = \int_0^{W_d} dz \int_0^{W} dy \int_0^{L} dx \left(1 - \frac{z}{W_d}\right) N_A(x,y,z)$$

Stolk et al., 1998

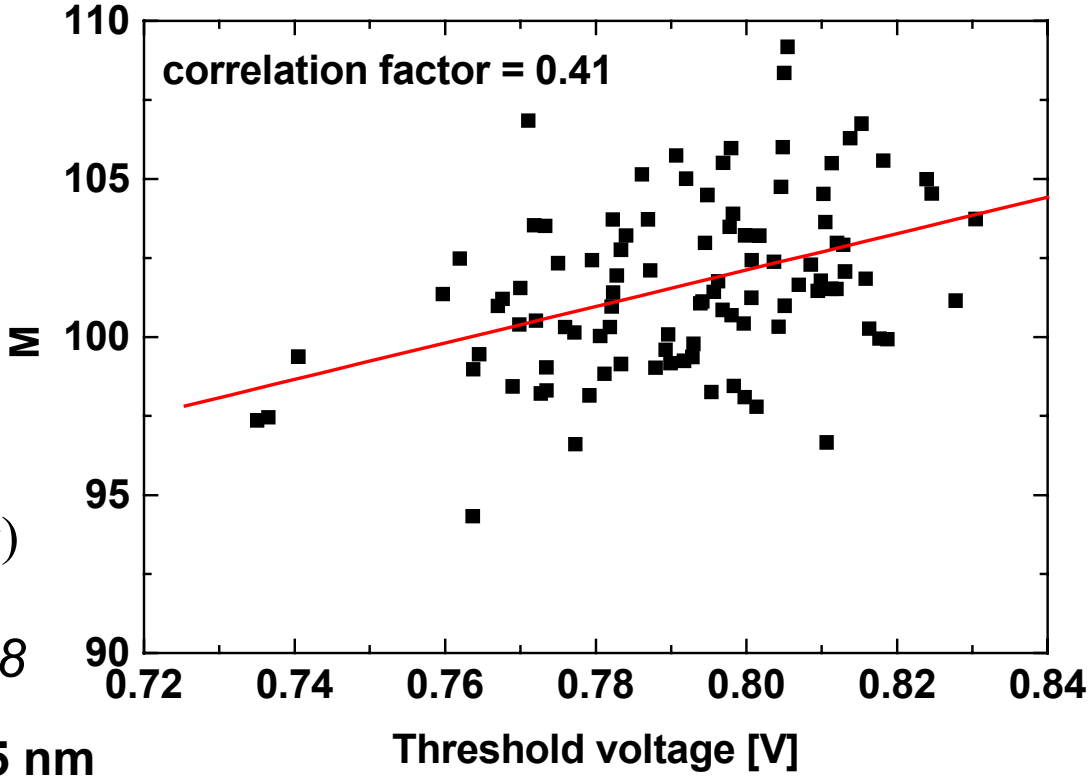

- L = 25 nm, W = 50 nm, W_d=15 nm

Distribution of V_T in Well tempered MOSFETs

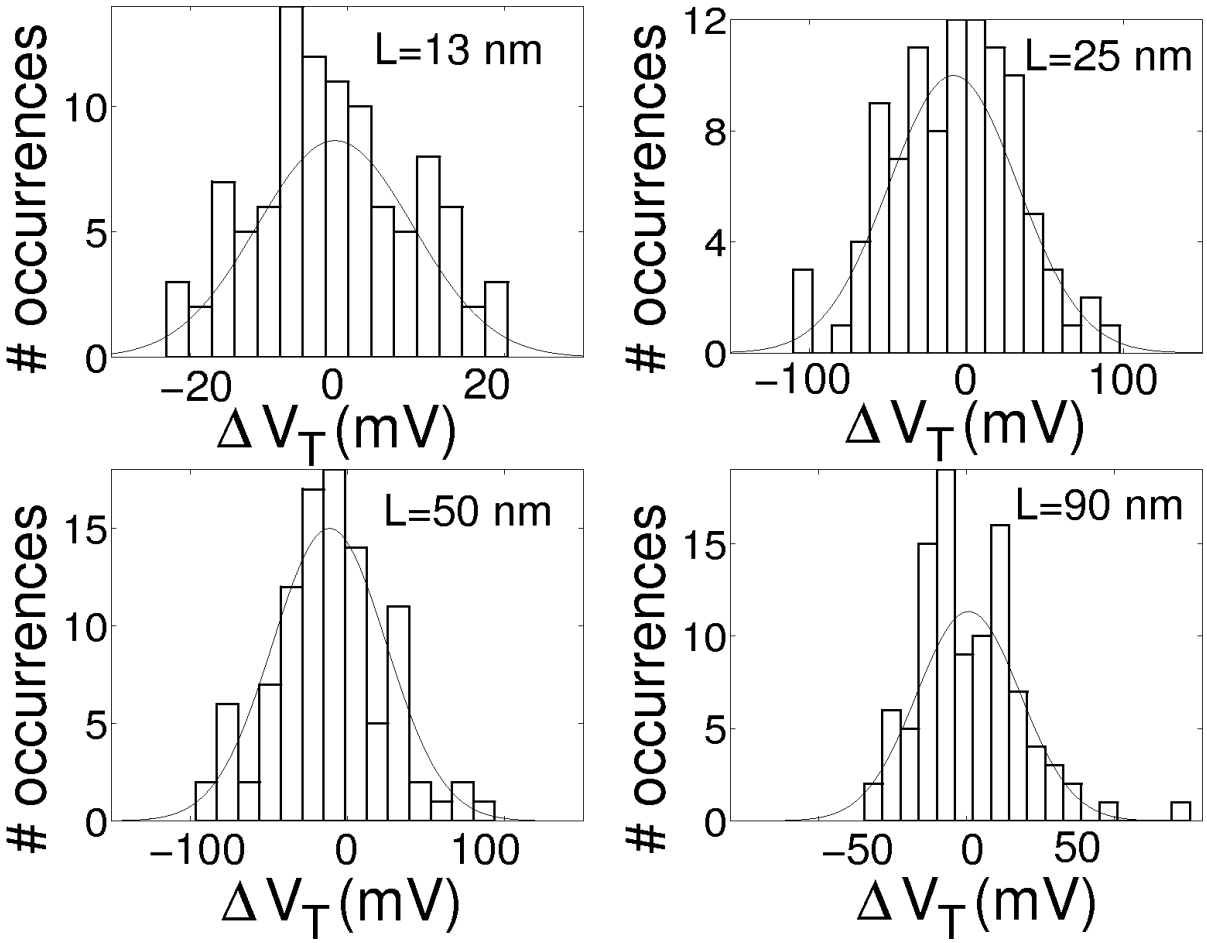

- **13 nm**
  - σ = 12.25 mV
  - $\langle V_T - V_{Tnom} \rangle$ = -1.6 mV
- **25 nm**
  - σ = 41 mV
  - $\langle V_T - V_{Tnom} \rangle$ = -8.3 mV
- **50 nm**
  - σ = 36.1 mV
  - $\langle V_T - V_{Tnom} \rangle$ = -11.4 mV
- **90 nm**
  - σ = 17.6 mV
  - $\langle V_T - V_{Tnom} \rangle$ = -0.72 mV

Standard deviation of V_T

L [nm]	ΔVT [mV]	σ1D [mV]	σ* 1D [mV]	σ3D sc [mV]	σ3D q [mV]
13	-1.6	17.3	40.7	6.9	12.25
25	-8.3	32	33	28.12	41
50	-11.4	14	14.9	23.29	36.1
90	0.72	21.1	23	14.86	17.6

Stolk et al. (1998)

Conclusion and future directions

- We have developed a code for the quantum simulation of nanoscale ballistic (and quasi-ballistic) MOSFETs
- In the considered MOSFETs the quantum confinement is relevant along the x direction, so we have solved the Schrödinger equation only in one dimension, with reduced computational requirements with respect to a full 2D or 3D quantum model.
- We need to validate the code with experimental results (the problem is to know the doping profiles).
- We are using the code as a design and evaluation tool of nanoscale MOSFETs, FinFETs, DG MOSFETs, Schottky barrier MOSFETs, Strained Si and SiGe MOSFETs
- Extend the capabilities of the code:
  - ✓ complete 2D and 3D solution of the Schrödinger equation
  - ✓ extract compact model parameters
  - ✓ Accelerate partially ballistic code